Chemical Engineering Science, Vol. 49, No. 4, pp. 469–480, 1994.
Printed in Great Britain.

0009–2509/94 $6.00 + 0.00

THE SIMULATED COUNTERCURRENT MOVING BED CHROMATOGRAPHIC REACTOR: A NOVEL REACTOR–SEPARATOR

AJAY K. RAY, ROBERT W. CARR† and RUTHERFORD ARIS
Department of Chemical Engineering and Materials Science, University of Minnesota, Minneapolis, MN 55455, U.S.A.

(*First received* 5 *February* 1993; *accepted in revised form* 17 *August* 1993)

Abstract—The simulated countercurrent moving bed chromatographic reactor (SCMCR) is a device for carrying out chemical reaction and separation simultaneously in a fixed bed. This is a novel reactor type in which separation takes place at the site of chemical reaction to improve product purities and conversions beyond those prescribed by thermodynamic equilibrium. The simulated countercurrent system mimics the behavior of a countercurrent moving bed by periodically changing feed and product locations sequentially along a fixed bed. The present investigations endeavor to determine to what extent the moving bed reactor advantages of high product purity and favorable equilibrium shifts are retained in SCMCR operations. An equilibrium stage model of the SCMCR consisting of a single fixed bed having a series of inlets and outlets along its length is considered. The mass balance equations are discretized to give an equilibrium plate model. Predictions of the concentration profiles in the column(s) are obtained for the 1,3,5-trimethylbenzene hydrogenation reaction at 463 K. It is shown that reaction and separation can be achieved simultaneously and that the yield of the reversible reaction can be improved greatly. Under appropriate operating conditions, the model calculations predict high-purity product streams and nearly complete conversion of a reaction which would otherwise be limited by equilibrium to 62%.

INTRODUCTION

In chromatographic reactors chemical reactions are carried out in the presence of a chromatographic stationary phase which separates the reactants and products from one another. The consequences of the reactive separation are that a high-purity product can be obtained, and an equilibrium-limited reaction can be forced toward completion. This allows one to carry out endothermic reactions at lower temperatures than normally would be employed due to the low equilibrium constant. A decrease in temperature will usually suppress side reactions and improve product quality, avoiding the need for further purification steps. Also, exothermic reactions with unacceptably low reaction rates at temperatures where the equilibrium yield is large could be run at higher temperatures and not be limited by low equilibrium conversions.

Reversible chemical reactions leading to the formation of more than one product can be favorably carried out in a continuous rotating annular chromatographic reactor (Cho *et al.*, 1980). The separation of the products inhibits the reverse step so that reactions with small equilibrium conversions can be driven to higher product yields. For reversible reactions of the type $A \rightleftharpoons B$ this general principle cannot be applied since there is only one product. However, if the reaction is heterogeneous, advantage can be taken of any difference in adsorption affinity of the reactant and product toward the solid phase to enhance the yield of the reaction (Cho *et al.*, 1982). The separation of the reactant and the product can be accomplished in a countercurrent moving bed or by simulating countercurrent movement between the solid and fluid. The reactant is fed into the fluid stream, and the reaction takes place on the solid.

Although several investigations of the countercurrent moving bed chromatographic reactor have recently appeared (Cho *et al.*, 1982; Petroulas *et al.*, 1985a, b; Fish *et al.*, 1986, 1988; Fish and Carr, 1989), there is very little reported work on the simulated countercurrent moving bed chromatographic reactor (SCMCR).

In order to preserve the advantages of countercurrent operation for the reversible reaction $A \rightleftharpoons B$ while avoiding the problems associated with movement of solids, it is convenient to simulate countercurrent motion. In the simulated moving bed the process aspects of the countercurrent moving bed are simulated by successively switching feed and product take-off streams through a series of inlets located at fixed intervals along a fixed bed. The fixed bed is divided into a number of segments with provision for adding feed to the stream passing from one segment to the next or of withdrawing a stream emerging from any segment. A shift of these positions in the direction of the fluid phase flow simulates movement of solids in the opposite direction, simulating continuous countercurrent flow of fluid and solid phases without actual movement of the solid. It is clear that the problems of solids handling, fines separation and flow channeling associated with the countercurrent moving bed are absent, while the advantages of countercurrency are retained. Furthermore, a smaller reactor volume is required because the bed expansion which occurs in a moving bed is absent, and since top and

†Author to whom correspondence should be addressed.

bottom reservoirs for feeding and collecting solids are not necessary, a smaller solids inventory can be maintained.

In this paper, a mathematical model of the SCMCR is developed and employed to investigate its performance. Input parameters that are characteristic of the catalytic hydrogenation of 1,3,5-trimethylbenzene, and that have been used in previous experimental and theoretical work on the countercurrent moving bed (Fish and Carr, 1989) are used to provide a basis for comparison of its performance with the SCMCR. The SCMCR predictions will be further tested in a forthcoming paper describing an experimental investigation of trimethylbenzene hydrogenation in a laboratory-scale SCMCR. Finally, to emphasize the purity and yield enhancement possible with the SCMCR, comparison is made with the predicted performance of a fixed bed tubular reactor operating without chromatographic separation.

Concerning the formulation of the model, it should be noted that the analysis and numerical solution constitutes by itself an interesting and challenging problem, because the concentration profiles inside the reactor may not reach a steady state in the time interval between successive changes of the inlet position. The reactor is always in a transient mode and the appropriate transient equations have to be solved. However, a periodic steady state with period equal to the inlet switching period will be eventually reached.

EQUILIBRIUM STAGE MODEL

The system is schematically represented in Fig. 1. The fixed bed of length L is divided into two sections. The portion of the reactor located between the feed point and the product take-off point will be identified as section I, while the remainder of the column will be designated as section II. The velocity of the fluid phase in section I is denoted by u_{I}, which is greater than u_{II}, the interstitial fluid-phase velocity in section II, by a factor of $1/\kappa$, where κ is the recycle fraction, $0 < \kappa < 1$. It was necessary to include recycle to obtain a converged solution to the mathematical model. Although it would not be necessary to employ recycle in experimental work, at some conditions, higher conversions are possible with it. The reactor is fitted with a series of inlets that are separated by a constant distance ΔL. The complete reactor is assumed to be formed by M segments of length ΔL. The number of segments for sections I and II are p and q, respectively. The corresponding lengths for both sections are L_{I} and L_{II}, so that

$$L = L_{\mathrm{I}} + L_{\mathrm{II}} = p\Delta L + q\Delta L = M\Delta L. \tag{1}$$

Sections I and II remain the same relative to the moving feed and product withdrawal points, but must be redefined with respect to the stationary column every time a switch is made. When the inlet position is advanced, the old and new segment numbers of sections I and II in Fig. 1 are related by eq. (2):

Before switching	*After switching*	
$(1)_{\mathrm{I}}$	$(q)_{\mathrm{II}}$	
$(e+1)_{\mathrm{I}}$	$(e)_{\mathrm{I}}$, $e = 1, 2, \ldots, (p-1)$	
$(1)_{\mathrm{II}}$	$(p)_{\mathrm{I}}$	(2)
$(f+1)_{\mathrm{II}}$	$(f)_{\mathrm{II}}$, $f = 1, 2, \ldots, (q-1)$.	

An equilibrium stage model incorporating the reaction scheme given by eq. (3) has been developed, where adsorption is described by a Langmuir isotherm:

$$A(\mathrm{g}) \underset{k_{dA}}{\overset{k_{aA}}{\rightleftharpoons}} A_{\mathrm{ads}} \underset{k_b}{\overset{k_f}{\rightleftharpoons}} B_{\mathrm{ads}} \underset{k_{dB}}{\overset{k_{aB}}{\rightleftharpoons}} B(\mathrm{g}). \tag{3}$$

Note that eq. (3) is a simplification, since the reaction occurs on different surface sites (Pt) than the selective adsorption for separation (Al_2O_3). The material balance equations for the fluid and solid phases for the reaction are then given by eqs (4) and (5):

$$\varepsilon\frac{\partial C_{ij}^m}{\partial t} + \varepsilon u_j\frac{\partial C_{ij}^m}{\partial L} + (1-\varepsilon)k_{ai}(N - n_{Aj}^m - n_{Bj}^m)C_{ij}^m - (1-\varepsilon)k_{di}n_{ij}^m = 0 \tag{4}$$

$$\frac{\partial n_{ij}^m}{\partial t} - k_{ai}(N - n_{Ai}^m - n_{Bj}^m)C_{ij}^m + k_{di}n_{ij}^m + \alpha_i(k_f n_{Aj}^m - k_b n_{Bj}^m) = 0 \tag{5}$$

where $i = \mathrm{A}$ or B, $j = \mathrm{I}$ or II, $m = 0, 1, 2, \ldots$, $\alpha_A = -1$ and $\alpha_B = 1$.

In eqs (4) and (5), C and n are, respectively, the fluid- and solid-phase concentration of component i for $mt_S < t < (m+1)t_S$ in section j. The suffix i is for component A or component B. The suffix j indicates the section number. The superscript m indicates the switching period for which the mass balance equations are being solved. The change in concentration in the axial direction around the nth stage is discretized

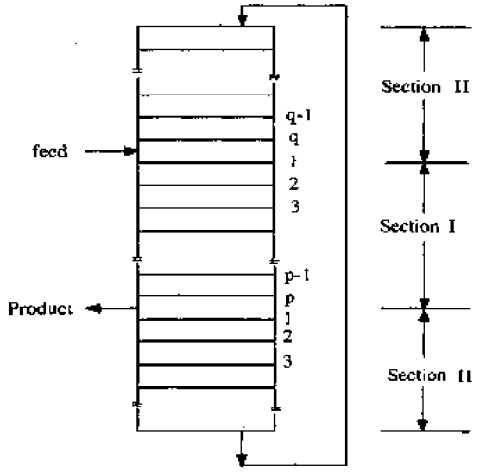

Fig. 1. Schematic diagram of simulated countercurrent moving bed reactor.

by eq. (6):

$$\frac{\partial C_{ij}^{m}(L_n, t)}{\partial L} = \frac{C_{ij}^{m}(L_n, t) - C_{ij}^{m}(L_{n-1}, t)}{\Delta L} \quad (6)$$

The subscript n is incorporated to discretize the mass balance equation for the mth switching period.

The two key parameters for simulated systems are the switching period, t_S, the time interval between successive advancements and the switching speed, ζ, the hypothetical or pseudo-linear flow rate of the solid phase. The switching period can be assumed to be constant and may conveniently be used as a characteristic time for the system. The dimensionless time can be defined as $\tau = t/t_S$. Therefore, the feed and take-off ports are advanced when $\tau = 1, 2, 3, \ldots$.

The switching speed, or the rate of switching, can be defined as the ratio of the length, ΔL, and the switching period:

$$\zeta = \frac{\Delta L}{t_S}. \quad (7)$$

The parameter $\sigma = [(1-\varepsilon)/\varepsilon]NKU_g/U_S$, which plays a key role in the CMCR, has a counterpart for the SCMCR defined by eq. (8), in which the solids speed U_S is replaced by the pseudo-speed ζ:

$$\sigma_i = \frac{1-\varepsilon}{\varepsilon} N_{\text{limiting adsorbate}} K_{\text{equilibrium},i} \frac{\zeta}{u_g}. \quad (8)$$

In the countercurrent moving bed, when $\sigma < 1$ component i travels with the gas phase, whereas when $\sigma > 1$ it travels with the solid phase at low concentration but with the gas phase at high concentration. In the countercurrent moving bed reactor system it has been observed that when reactant A travels with the solid phase ($\sigma_A > 1$) and product B travels with the gas phase ($\sigma_B < 1$), separation between reactant and product can enhance the conversion of reactant and the purity of the product. Similar conditions can be derived for simulated countercurrent moving bed reactor systems if we visualize ζ as the pseudo-velocity of the solid phase. Separation can be accomplished in the reactor by adjusting U_g and ζ such that $\sigma < 1$ for one component and $\sigma > 1$ for the other. If the reactant travels more slowly than the feedpoint, its residence time and hence the conversion will increase. If, at the same time, the product travels with the mobile phase, separation can be achieved and an improved product purity can be obtained. This can be realized by adjusting U_g and ζ. Thus, an observer located at the feed point will observe countercurrent separation of components A and B.

Dimensionless variables and parameters are defined as follows [eq. (9)]:

$$\gamma_{ij}^{m} = K_i C_{ij}^{m}, \quad \upsilon_{ij}^{m} = \frac{n_{ij}^{m}}{N}, \quad \xi_n = \frac{L_n}{L_j}, \quad \tau = \frac{t}{t_S},$$

$$K_i = \frac{k_{ai}}{k_{di}}, \quad K_r = \frac{k_f}{k_b}, \quad \beta_j = \frac{\zeta}{u_j}; \quad \mu_i = \frac{1-\varepsilon}{\varepsilon} NK_i \quad (9)$$

$$\lambda_i = \mu_i k_{di} t_S, \qquad \delta_i = \mu_i k_f t_S$$

where $i = $ A or B, $j = $ I or II, $m = 0, 1, 2, \ldots$, and $n = 1, 2, 3, \ldots, p$ for section I, $n = 1, 2, 3, \ldots, q$ for section II.

The mass balance equations (4) and (5) were discretized using eq. (6) to give the equilibrium stage model. The discretized mass balance equation in dimensionless form is given by eqs (10) and (11):

$$\frac{d\gamma_{ij}^{m}}{d\tau} = \frac{1}{\beta_j}[\gamma_{ij}^{m}(\xi_{n-1}, \tau) - \gamma_{ij}^{m}(\xi_n, \tau)] - \lambda_i[(1 - \upsilon_{Aj}^{m} - \upsilon_{Bj}^{m})\gamma_{ij}^{m} - \upsilon_{ij}^{m}] \quad (10)$$

$$\mu_i \frac{d\upsilon_{ij}^{m}}{d\tau} = \lambda_i[(1 - \upsilon_{Aj}^{m} - \upsilon_{Bj}^{m})\gamma_{ij}^{m} - \upsilon_{ij}^{m}] + \alpha_i \delta_i \left[\upsilon_{Aj}^{m} - \frac{\upsilon_{Bj}^{m}}{K_r}\right] \quad (11)$$

where $i = $ A or B, $j = $ I or II, $m = 0, 1, 2, \ldots$, and $\alpha_A = -1$, $\alpha_B = 1$.

The boundary conditions are specified as follows. The inlet stream to section I consists of a mixture of the outlet stream from section II and the feed stream. A mass balance around the feed point considering no accumulation results in eq. (12):

$$\gamma_{i,\mathrm{I}}^{m}(0, \tau) = \kappa\gamma_{i,\mathrm{II}}^{m}(1, \tau) + (1-\kappa)\gamma_{i,f} \quad (12)$$

where $i = $ A or B, $\gamma_{i,f}$ is the dimensionless feed concentration of component i. If the feed contains only reactant A, then $\gamma_{B,f} = 0$.

At the product take-off points, if we assume the concentration to be continuous, then

$$\gamma_{i,\mathrm{I}}^{m}(1, \tau) = \gamma_{i,\mathrm{II}}^{m}(0, \tau), \quad i = \text{A or B}. \quad (13)$$

The fluid- and solid-phase concentrations are related through the Langmuir isotherm by

$$\upsilon_{ij}^{m}(\xi_n, \tau) = \frac{\gamma_{ij}^{m}(\xi_n, \tau)}{1 + \gamma_{Aj}^{m}(\xi_n, \tau) + \gamma_{Bj}^{m}(\xi_n, \tau)} \quad (14)$$

where $i = $ A or B, $j = $ I or II, $m = 0, 1, 2, \ldots$.

The specification of the initial conditions is very important for the solution of this problem and it is necessary to explain in detail the procedure that establishes it. It should be first noted that the solution has to be constructed sequentially. If we want to calculate the concentration profiles of component i in the time interval between the mth and $(m+1)$th advancements (i.e. for $m \leqslant \tau \leqslant m+1$, $m = 0, 1, 2, \ldots$), then it is required to solve the mass balance equations for $\gamma_{ij}^{m}(\xi_j, \tau)$. However, since the switching period is constant between successive advancements and equal to 1 (in terms of τ), it is sufficient if we solve these equations for $0 \leqslant \tau \leqslant 1$. The initial conditions for the mth interval can be obtained from the concentration profiles of sections I and II that are present just before the mth switching. Hence, the initial conditions are calculated from eq. (15):

$$\gamma_{ij}^{m}(\xi_n, 0) = \gamma_{ij}^{m-1}(\xi_n, 1), \quad m = 1, 2, 3, \ldots. \quad (15)$$

Equations (1)–(15) completely define the simulated countercurrent chromatographic reactor and concen-

tration profiles can be obtained from the solution of the mass balance equations by a fourth-order Runge–Kutta method. The computations were done on a Cyber model 180-825 computer, and required between 32 and 85 CPU units, depending upon the time step and the final time.

MODEL REACTION

Reactions for which the CMCR and SCMCR would be advantageous should have the following characteristics: (1) It should be a catalytic reaction of the form $A \rightleftharpoons B$. Reactions of the form $A + C \rightleftharpoons B$ or $A \rightleftharpoons B + C$ can be used if the kinetics are zeroth order with respect to C, or if C is present in sufficient excess that it is not separated from A or B and the kinetics are pseudo-first-order with respect to A or B, respectively. (2) The forward reaction rate constant should be fairly large. (3) Both the forward and backward reactions should take place on the solid phase only. (4) There should be an equilibrium limitation on the yield of B. (5) Side reactions on the solid or fluid phase should be avoided as much as possible. (6) The product and the reactant must have different chromatographic properties. The relative adsorbability should be large enough for a good separation. In other words, we expect both components A and B to be chromatographically separable. (7) The solid phase supporting the catalyst should be stable, have high capacity and a favorable adsorption isotherm.

Good possibilities for a test system are reactions in which there is a rearrangement of a group of bonds to produce an isomer of the reactant, or disappearance of a characteristic group and formation of another. The disadvantages of many reactions will be the formation of side products which may affect the purity of the desired product.

The Pt-catalyzed hydrogenation of mesitylene (1,3,5-trimethylbenzene) to 1,3,5-trimethylcyclohexane (TMC) was identified as adequately fulfilling the above conditions, and was selected as a suitable test reaction for the CMCR (Petroulas *et al.*, 1985b). The reaction is exothermic, with $\Delta H = -196.6$ kJ mol^{-1}. Over the temperature range for which equilibrium favors the dehydrogenation step, the reaction is very clean, giving TMC as the only product. In the vicinity of 463–473 K reaction rates are suitable and the reaction is equilibrium limited. In a nonseparative reactor the equilibrium conversion of mesitylene in excess H_2 (25% v/v in the N_2 carrier) is about 40% at 473 K and 62% at 463 K (Egan and Buss, 1959). This is the appropriate temperature region for the experimental study since at higher or lower temperatures the reaction is practically irreversible with equilibrium favoring mesitylene or trimethylcyclohexane, respectively. Mesitylene dehydrogenation is an appropriate choice for SCMCR investigations not only for these reasons, but also since it will allow comparisons with the CMCR (Fish *et al.*, 1989).

Egan and Buss (1959) reported the forward reaction rate constant for the Pt-catalyzed hydrogenation of mesitylene, $k_f = 0.09\ s^{-1}$, and the equilibrium constant $K_r = K_f/k_b = 128$, both at 463 K. Also, the adsorption equilibrium rate constant for mesitylene, $K_A = k_{aA}/k_{dA} = 4.84$, and the adsorption equilibrium rate constant ratio for mesitylene and trimethylcyclohexane, $K = K_A/K_B = 4.0$, are available (Petroulas, 1984). The adsorption rate constant for mesitylene, k_{aA}, and for trimethylcyclohexane, k_{aB}, were estimated to each be approximately 200 cm s^{-1}.

RESULTS AND DISCUSSION

Concentration profiles were obtained from the solution of the discretized mass balance equations (10) and (11). Although the reactor is always in a transient mode, a periodic steady state with a period equal to the switching period is eventually reached. The predicted steady-state axial gas-phase concentration profile of mesitylene is shown in Fig. 2 for a reactor divided into 20 stages with 8 stages in section I and switching periods of 5 s. It can be seen that the concentration profiles at these equal instants of time,

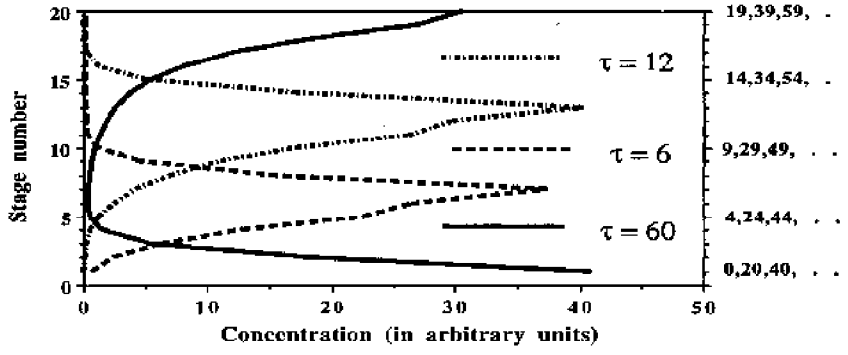

Fig. 2. Reactant concentration profile for different values of τ. Feed points at stage 7 ($\tau = 6$), stage 13, ($\tau = 12$), and stage 1 ($\tau = 60$). $p = 8$; $q = 12$; $t_s = 5$ s; $\zeta = 4$; $u_g = 5$ cm/s; $\kappa = 0.85$; $\sigma_A = 1.2$; $\sigma_B = 0.3$; conversion = 0.997; purity = 98.5%.

which are just before the next advancement of the feedpoint, are virtually the same. Since the profile has relaxed into this waveform during a switching period, it can be considered to be a periodic steady state. In these calculations the length of the reactor was 400 cm, 15% of the fluid stream was withdrawn as product 9 stages ahead (in the direction of mobile-phase flow) of the feed entry point, and the remainder was recycled. Make-up feed (15%) is mixed with the recycle stream at the feed inlet. Functionally, the reactor has no top or bottom and the inlet and outlet positions can be moved around the reactor bed continuously, always with the same distance between the various streams. All the calculations are at low feed concentration ($\gamma_{Af} = 0.1$, $\gamma_{Bf} = 0.0001$), so that the adsorption isotherms are linear. The phase ratio parameter for mesitylene, μ_A, was 1.75, and $\sigma_A = 1.2$ and $\sigma_B = 0.3$.

In all the calculations, the integration step size $\Delta\tau$ was 0.001 s. When the value of $\Delta\tau$ was increased from 0.001 to 0.005 s keeping all other parameters at their reference values, the solution of the mass balance equations for the concentration profiles became numerically unstable because steep concentration fronts are formed and move through sections upon switching. When $\Delta\tau$ was decreased from the reference value of 0.001 to 0.0005 s, almost identical concentration profiles to those in Fig. 2 were obtained, justifying the choice of $\Delta\tau = 0.001$ s.

In Fig. 2, the y-axis scale on the left indicates the stage number, and the corresponding numbers on the right indicate values of the characteristic time τ for which stages 1, 5, 10, 15, and 20 are the feed plate. This figure illustrates propagation of mesitylene concentration profiles along the reactor giving their position after $\tau = 6$ (feed plate 7, product take-off plate 15), $\tau = 12$ (feed plate 13, product take-off plate 1) and $\tau = 60$ (feed plate 1, product take-off plate 9). The progression of trimethylcyclohexane concentration profiles along the reactor by giving their position after 6, 12, and 60 switching periods is shown in Fig. 3 for operating parameters similar to Fig. 2. Figure 4 shows the concentration profile of both MES and TMC along the reactor for $\tau = 60$. In this figure, the feed enters on plate 1 and product is taken off at plate 9. From this figure we can see that if

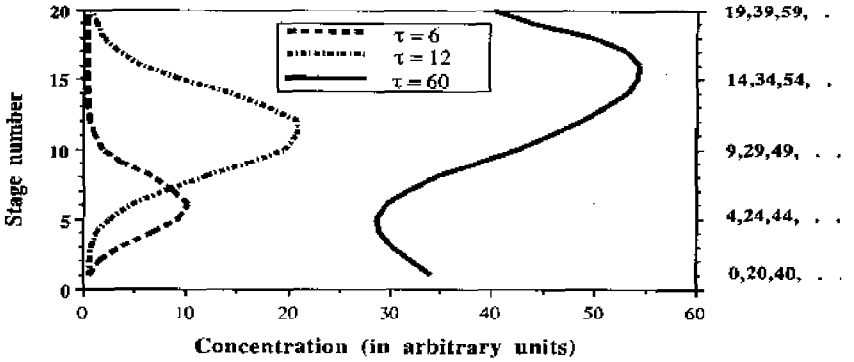

Fig. 3. Product concentration profile for different values of τ. Product removal at stage 15 ($\tau = 6$), stage 21 ($\tau = 12$), and stage 9 ($\tau = 60$). $p = 8$; $q = 12$; $t_S = 5$ s; $\zeta = 4$; $u_s = 5$ cm/s; $\kappa = 0.85$; $\sigma_A = 1.2$; $\sigma_B = 0.3$; conversion = 0.997; purity = 98.5%.

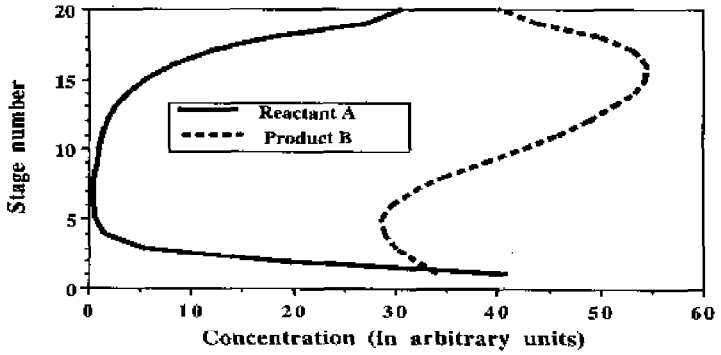

Fig. 4. Steady-state concentration profile for reactant and product. Feed enters on stage 1, product removal on stage 9. $p = 8$; $q = 12$; $t_S = 5$ s; $\zeta = 4$; $u_s = 5$ cm/s; $\kappa = 0.85$; $\sigma_A = 1.2$; $\sigma_B = 0.3$; conversion = 0.997; purity = 98.5%.

the product is withdrawn around stage 9 a highly purified product stream can be obtained. Under these operating conditions the conversion was nearly unity (0.977) and the product purity was 98.5%. The equilibrium conversion for the reaction in a nonseparative reactor at 190°C is 0.62.

Figure 5 shows the effect of increasing the switching period and thereby the effect of decreasing the solid pseudo-flow rate. In this figure, steady-state concentration profiles of reactant and product were obtained for the switching period of 10 s, and the solids pseudo-speed was subsequently decreased from 4 to 2 cm s^{-1} giving $\sigma_A = 1.167$ and $\sigma_B = 0.29$. By increasing t_S to 10 s, it is not possible to maintain $\sigma_A > 1$ and $\sigma_A < 1$. To achieve that one has to change either ΔL or u_g. In Fig. 5, u_g was decreased to 3 from 5, ΔL left at 20, but L was increased from 400 to 500, resulting in an increase in the number of stages from 20 to 25. In the calculation, 15% of the fluid stream was withdrawn as product from the 11th stage from the feed entry point and the remainder was recycled. Both MES and TMC are distributed along the entire reactor length. In this case as the reactant residence time increases, so does the conversion. In addition, with low solids flow rate, the reactant has decreased to a low value at the product take-off point, giving a better product purity. The conversion and product purity are 0.9984 and 99.34%, respectively. The appearance of more product and less reactant in section II is because more product is formed due to the longer residence time

Figure 6 shows the effect of increasing the solids pseudo-flow rate to 5 cm s^{-1} by increasing the switching length while keeping the switching period constant at 5 s. At these conditions, $\sigma_A = 1.75$ and $\sigma_B = 0.438$. In this case, the MES travels relatively faster than in the earlier cases, more reactant is present at the take-off point, and product purity deteriorates. The higher solids pseudo-flow rate shortens the reactant residence time sufficiently that the conversion also decreases, and there is reactant present in section II. The conversion and product purity in this case are only 0.981 and 98.36%, respectively.

Figure 7 shows the effect of increasing the reactor length. In this case the length was doubled, with 20 segments in section I and 30 segments in section II,

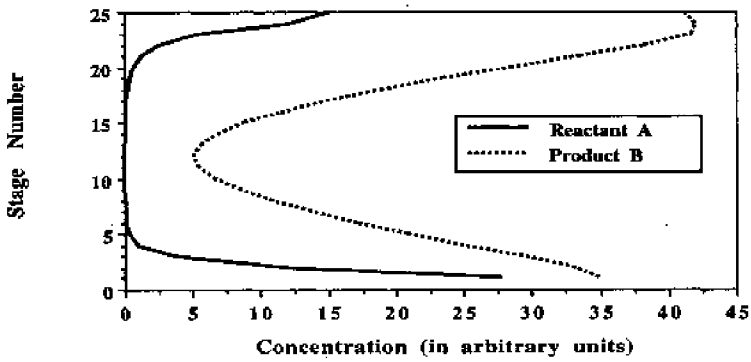

Fig. 5. Steady-state concentration profile for reactant and product. Feed enters on stage 1, product is removed on stage 11. $p = 10$; $q = 15$; $t_S = 10$ s; $\zeta = 2$; $u_g = 3$ cm/s; $\kappa = 0.85$; $\sigma_A = 1.17$; $\sigma_B = 0.29$; conversion = 0.9984; purity = 99.34%.

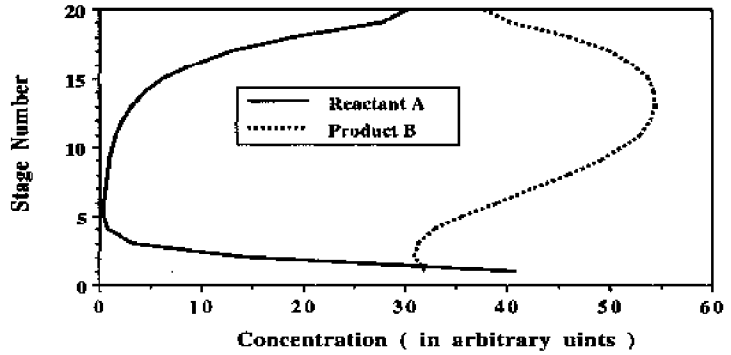

Fig. 6. Steady-state concentration profile for reactant and product. Feed enters on stage 1, product is removed on stage 13. $p = 8$; $q = 12$; $t_S = 5$ s; $\zeta = 5$; $u_g = 5$ cm/s; $\kappa = 0.85$; $\sigma_A = 1.75$; $\sigma_B = 0.44$; conversion = 0.981; purity = 98.36%.

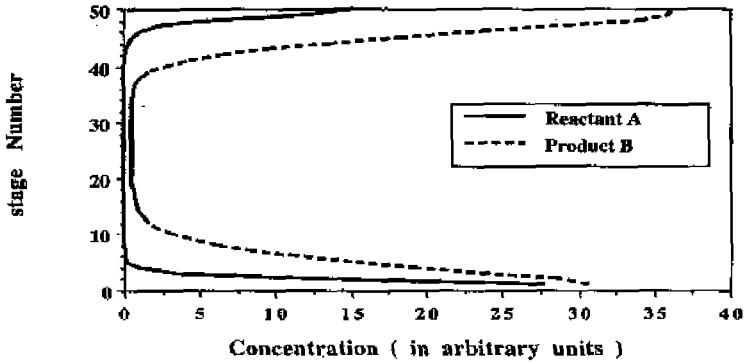

Fig. 7. Steady-state concentration profile for reactant and product. Feed enters on stage 1, product is removed on stage 21. $p = 20$; $q = 30$; $t_S = 10$ s; $\zeta = 2$; $u_g = 3$ cm/s; $\kappa = 0.85$; $\sigma_A = 1.17$; $\sigma_B = 0.29$; conversion = 0.9997; purity = 99.22%.

Table 1. % purity and % conversions obtained for various values of σ_A and σ_B, switching time (t_S), recycle ratio ($1 - \kappa$), inlet feed concentration (γ_{Af}), pseudo-solid velocity (ζ) and length of the reactor (L)

Run no.	σ_A	σ_B	t_S	$1-\kappa$	γ_{Af}	ζ	L	% purity	% conversion
1	1.2	0.3	5	0.15	0.1	4	400	98.50	99.70
2	1.167	0.29	10	0.15	0.1	2	500	99.34	99.84
3	1.75	0.4375	5	0.15	0.1	5	500	98.36	98.10
4	1.167	0.29	10	0.15	0.1	2	1000	99.22	99.97
5	1.75	0.4375	5	0.5	0.1	5	500	93.83	91.60
6	1.75	0.4375	5	0.15	5.0	5	500	95.92	97.90
7	1.2	0.3	5	0.25	0.1	5	500	95.60	99.10
8	2.0	0.5	5	0.15	0.1	5	500	96.30	98.40
9	2.0	0.5	5	0.25	0.1	5	500	93.30	98.20
10	1.75	0.4375	5	0.15	1.0	5	500	97.82	98.10

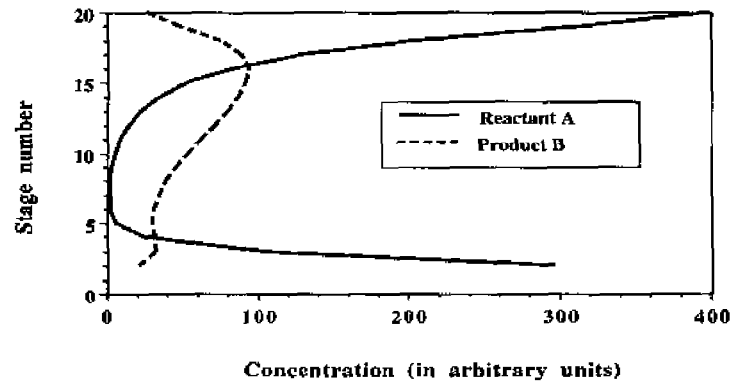

Fig. 8. Steady-state concentration profile for reactant and product. Feed enters on stage 1, product is removed on stage 7. $p = 8$; $q = 12$; $t_S = 5$ s; $\zeta = 5$; $u_g = 5$ cm/s; $\kappa = 0.50$; $\sigma_A = 1.75$; $\sigma_B = 0.44$; conversion = 0.916; purity = 93.83%.

and $\Delta L = 20$. In the calculation, 15% of the fluid stream was withdrawn as product from the 21st stage from the feed entry point and the remainder was recycled. The switching time was set at 10 s, resulting in the values of $\sigma_A = 1.167$ and $\sigma_B = 0.29$. The longer reactor length increases the MES residence time, resulting in higher conversion. The conversion under these operating conditions increases to 0.999 and the product purity is 99.2%.

Figure 8 shows the effect of increasing the feed rate. In all the previous calculations the concentration profiles were obtained for an 85% recycle ratio. In this case the make-up feed rate was increased from 15 to 50%. In attempting to increase productivity by in-

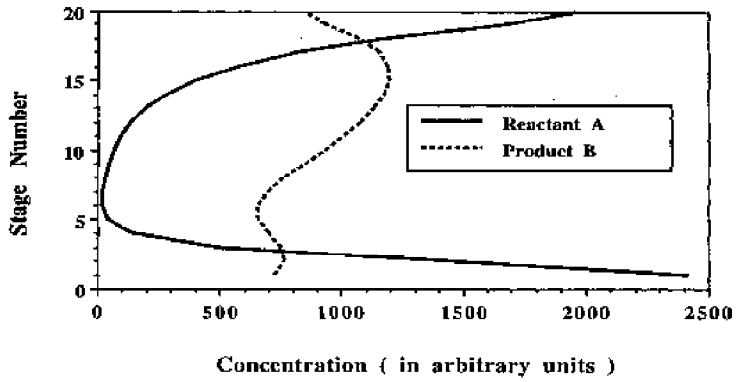

Fig. 9. Steady-state concentration profile for reactant and product. Feed enters on stage 1, product is removed on stage 7. $p = 8$; $q = 12$; $t_S = 5$ s; $\zeta = 5$; $u_g = 5$ cm/s; $\kappa = 0.85$; $\gamma_{Af} = 5$; $\sigma_A = 1.75$; $\sigma_B = 0.44$; conversion = 0.979; purity = 95.92%.

creasing the feed rate, it is necessary to increase the solids flow rate even though it will decrease the conversion. The switching period was set at 5 s, thereby giving a pseudo-solid velocity of 5 cm·s^{-1}. The values of the relative carrying capacity parameter (σ) are 1.75 and 0.438. The conversion and product purity are reduced to 0.916 and 93.8%, respectively, showing the combined effects of feed rate and recycle ratio.

Figure 9 shows the effect of increasing the feed concentration. In this case, the feed concentration was increased by 50 times to $\gamma_{Af} = 5.0$. The high feed concentration may force the solid-phase concentration to approach the nonlinear region of the adsorption isotherm. The effect of this may lead to flooding the column to the point where, by analogy with the CMCR, and product purity deteriorates. The conversion and product purity under the high feed condition are 0.979 and 95.9%, respectively.

Table 1 shows the conversion and product purity obtained for different sets of the parameters σ_A and σ_B, switching time (t_S), inlet feed concentration (γ_{Af}), recycle ratio ($1 - \kappa$), pseudo-solid velocity (ζ), and length of the reactor (L). The performance figures in the table compare very favorably with the predicted performance of the CMCR according to a linear model, as well as the observed performance of a laboratory-scale CMCR (Fish and Carr, 1989), all for the same reaction/catalyst/adsorbent system. A detailed comparison is not possible, however, because of some differences in input parameters for the calculations.

COMPARISON OF THE SIMULATED MOVING BED WITH FIXED BED OPERATION

Mathematical models of a continuous flow fixed bed reactor and the simulated countercurrent moving bed will be considered to compare the product purity and conversion of an equilibrium-limited reversible first-order reaction of the type A⇌B. In both reactors, there are P plates or stages. In the fixed bed reactor, feed enters at the top of the bed (on plate 1) and product is collected at the bottom of the reactor (plate P). The simulated bed is fitted with inlets and outlets at each plate with provision of adding feed or withdrawing product streams. The feed entry point is switched successively through each stage in sequence keeping the product take-off point always P plates ahead of the feed entry plate. The bed has no top or bottom and feed and product streams are switched in cycles.

Similar material balance equations can be written for both the fixed bed and simulated bed systems following the reaction scheme given by eq. (3). The dimensionless form of the material balance equations for the fluid and solid phases is then given by

Fixed bed:

$$\frac{d\gamma_i}{d\tau_1} = P[\gamma_i(\xi_{m-1}, \tau_1) - \gamma_i(\xi_m, \tau_1)] - \lambda_i[(1 - \upsilon_A - \upsilon_B)\gamma_i - \upsilon_i] \quad (16)$$

$$\mu_i \frac{d\upsilon_i}{d\tau_1} = \lambda_i[(1 - \upsilon_A - \upsilon_B)\gamma_i - \upsilon_i] + \alpha_i\delta_i\left(\upsilon_A - \frac{\upsilon_B}{K_r}\right) \quad (17)$$

Simulated moving bed:

$$\frac{d\gamma_i}{d\tau_2} = \frac{1}{\beta}[\gamma_i(\xi_{m-1}, \tau_2) - \gamma_i(\xi_m, \tau_2) - \lambda_i[(1 - \upsilon_A - \upsilon_B)\gamma_i - \upsilon_i] \quad (18)$$

$$\mu_i \frac{d\upsilon_i}{d\tau_2} = \lambda_i[(1 - \upsilon_A - \upsilon_B)\gamma_i - \upsilon_i] + \alpha_i\delta_i\left(\upsilon_A - \frac{\upsilon_B}{K_r}\right) \quad (19)$$

where

$$\tau_1 = \frac{t}{(L/u_g)} \quad \text{and} \quad \tau_2 = \frac{t}{t_S}.$$

The initial value equations were solved by the fourth-order Runge–Kutta method to obtain the outlet concentration of reactant and product. The adsorption–desorption and reaction rate constants were as

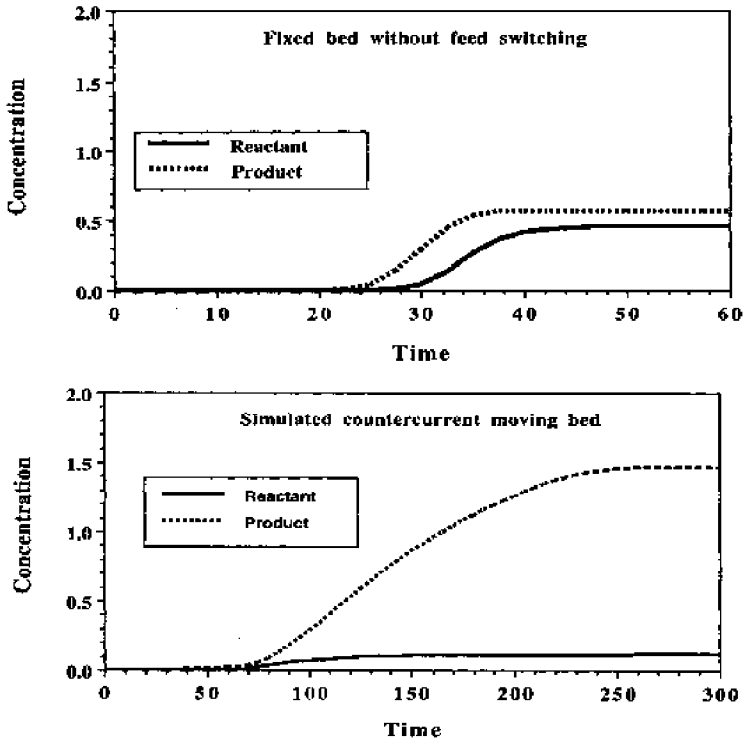

Fig. 10. Concentration profile of reactant and product with time for a fixed bed system and for a simulated moving bed system (total plates = 25; carrier flow rate = 10; switching time = 10). Fixed bed: conversion = 0.575; product purity = 55.46%; simulated moving bed: conversion = 0.896; purity = 92.91%.

in the previous section. Figures 10–13 show the results of such calculations. These figures also show the breakthrough time of the reactant and product for the various parameter values.

Figure 10 shows the concentration profile of reactant and product with time at the exit of the column for both a continuous fixed bed system and a simulated countercurrent moving bed system. In this figure, concentration profiles were obtained for a column containing 25 plates and for a carrier gas velocity of 10 cm s^{-1}. For the simulated moving bed system, a switching time of 10 s was assumed. The figure distinctly shows the advantage of the simulated moving bed with respect to both conversion and product purity. The conversion is calculated from the ratio of total moles of product collected to the total moles of feed entering the column in that span of time. The conversion and product purity for the fixed bed system are 57.5 and 55.46%, respectively, while for the SCMCR the conversion and product purity are 89.6 and 92.91%, respectively.

Figure 11 shows similar output concentration profiles for a carrier gas velocity of 5 cm s^{-1}, all other conditions remaining unchanged. With slow carrier flow rate, the breakthrough times of the reactant and product are longer. Also, in this case the residence time of the reactant is greater, and therefore the conversion and product purity are also higher. The conversion and product purity for the fixed bed system are 61.7 and 60.53%, respectively, while for the SCMCR the conversion and product purity are 92.4 and 96.1%, respectively.

Figure 12 shows the effect of decreasing the switching time and thereby of increasing the pseudo-solid flow rate. In this figure, the concentration profile with time at the exit of the bed is shown for the SCMCR for a 5 s switching time keeping all other parameter values unchanged. The concentration profile shown in the top half of Fig. 12 is the same as that of the top half of Fig. 10 as conditions for calculation of fixed bed are identical. With higher solids flow rate, the reactant residence time decreases and so does the conversion. In addition, both the reactant and product are distributed along the length of the bed, except in this case the concentration of reactant present at the exit is larger, deteriorating the product purity. For the SCMCR the conversion and product purity are 84.8 and 85.96%, respectively.

To investigate the effect of the degree of subdivision of the bed, numerical simulation was done for a reactor containing 10 plates. Figure 13 shows the concentration profiles. Qualitative argument for this figure is similar to Fig. 12 as in this case the pseudo-solid velocity is higher than that of the conditions for

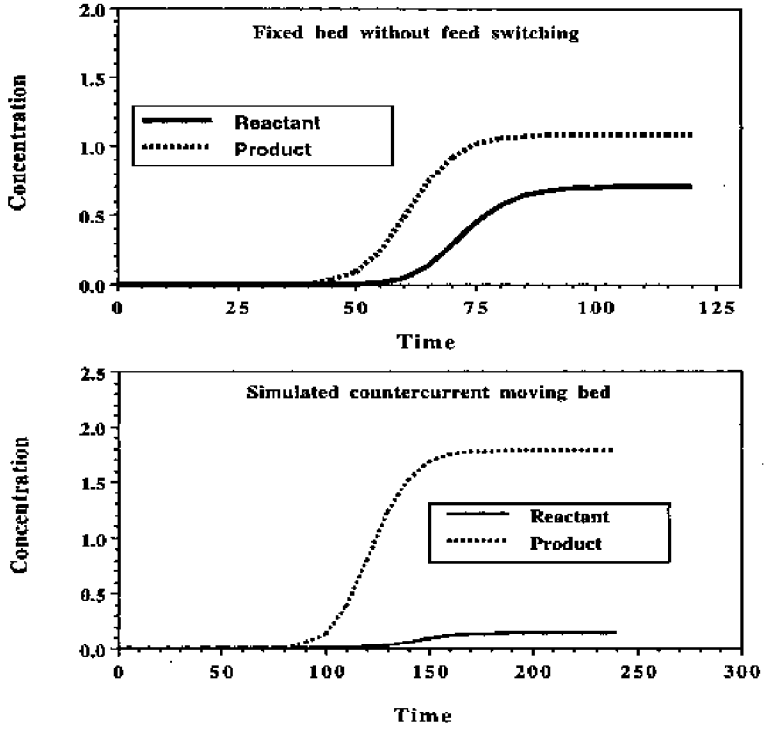

Fig. 11. Concentration profile of reactant and product with time for a fixed bed system and for a simulated moving bed system (total plates = 25; carrier flow rate = 5; switching time = 10). Fixed bed: conversion = 0.617; product purity = 60.53%; simulated moving bed: conversion = 0.924; purity = 96.1%.

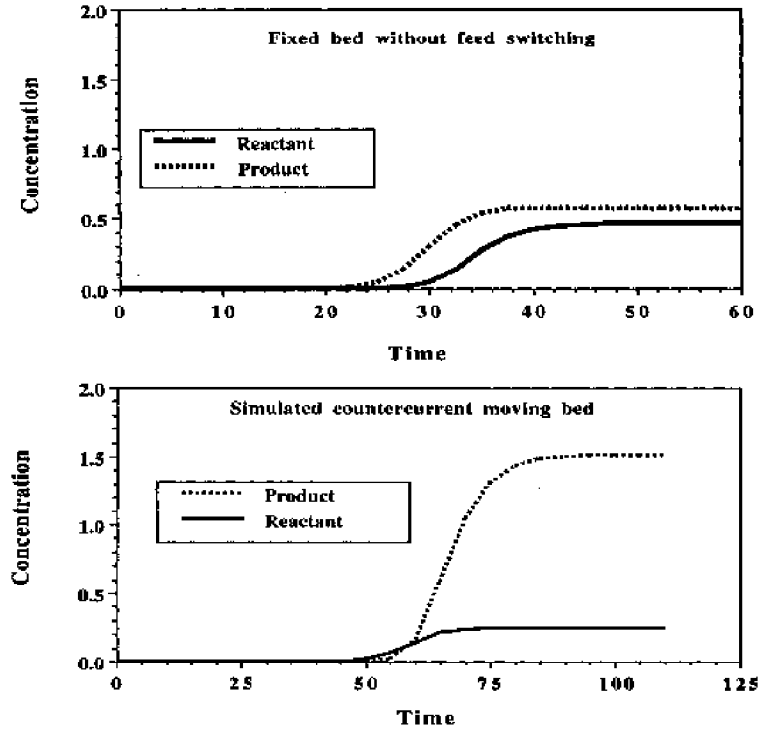

Fig. 12. Concentration profile of reactant and product with time for a fixed bed system and for a simulated moving bed system (total plates = 25; carrier flow rate = 10; switching time = 5). Fixed bed: conversion = 0.575; product purity = 55.46%; simulated moving bed: conversion = 0.848; purity = 85.96%.

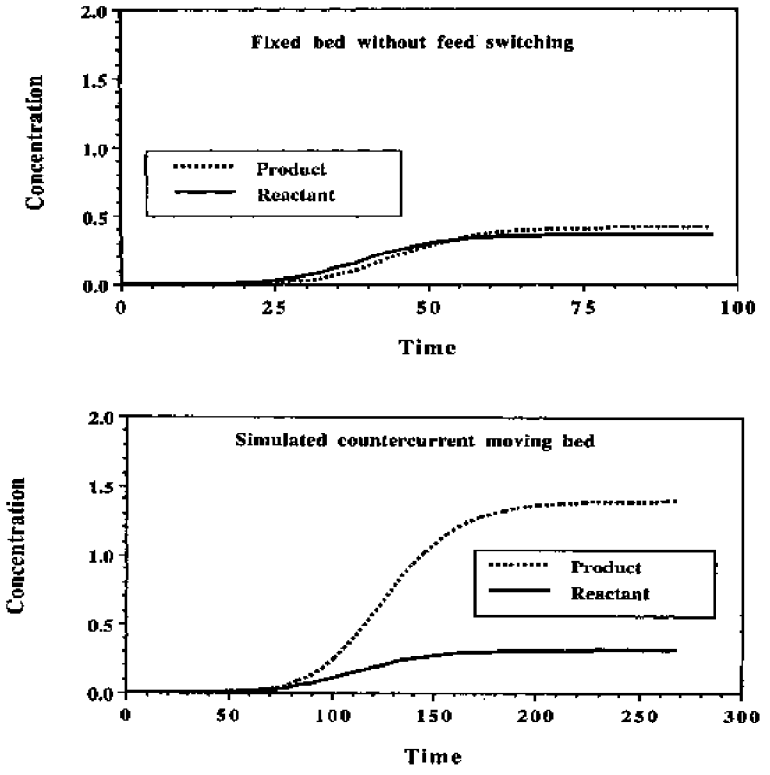

Fig. 13. Concentration profile of reactant and product with time for a fixed bed system and for a simulated moving bed system (total plates = 10; carrier flow rate = 10; switching time = 10). Fixed bed: conversion = 0.521; product purity = 53.37%; simulated moving bed: conversion = 0.837; purity = 82.04%.

Fig. 10. Even though the switching time is constant at 10 s, the switching length is longer as fewer number of plates are required for the same reactor length. Thus, the conversion and product purity are expected to be lower than that of Fig. 10. The conversion and product purity for the fixed bed system are 52.1 and 53.37%, respectively, while for the simulated moving bed system conversion and product purity are 83.7 and 82.04%, respectively.

The improved conversion and product purity obtained in the SCMCR can be explained from the concentration profiles of reactant and product with time in Figs 10–13 for a fixed bed. It can be seen that in the vicinity of reactant and product breakthrough, the product purity is very high. The improved performance of the SCMCR results from taking advantage of this by switching the feed position around the breakthrough point of the reactant and product.

The theoretical analysis predicts better conversion and product purity with the SCMCR than with the traditional fixed bed reactor for reversible reactions that are first order in both directions provided the reactant and product are separable. For an equilibrium limited reaction, the exit concentration for a fixed bed reactor reaches the equilibrium value whereas improved exit product concentration can be obtained in the SCMCR, and conversion can be increased beyond the thermodynamic equilibrium value of a nonseparative reactor. The product can be made highly pure under proper operating conditions, eliminating or greatly reducing the need for further processing steps to purify the products.

CONCLUSION

A systematic and generalized model for the simulated countercurrent moving bed reactor system, and analysis of the solution of the mathematical model has been discussed. A single fixed bed with a series of feed ports along its length was considered. The continuous feedstream is switched from one inlet to the next in order to achieve relative movement between the feed and the bed, thus simulating the fixed feed countercurrent moving bed chromatographic reactor, although in discrete steps. However, the simulated system poses a new and challenging theoretical problem for reactor modeling, since each time the feedstream is switched a transient state is created which relaxes toward steady state, only to be interrupted by another switch. A simple equilibrium stage model with the assumption that concentrations are uniform in each stage reduces the partial differential equations to ordinary differential equations that are numerically solved by the fourth-order Runge–Kutta method. A chemical reaction of the type $A \rightleftharpoons B$ with linear kinetics and Langmuir adsorption equilibrium isotherm is studied. Various dimensionless vari-

ables and parameters that control the overall performance of the reactor have been identified, and the conditions that have to be satisfied in order to simulate the separation capabilities of the actual countercurrent moving bed reactor have been established. The model predicted product purities over 99% and conversion near unity for the mesitylene hydrogenation reaction for which equilibrium conversion is 62%.

The characteristics and reactor behavior of a long single column fixed bed are compared with those of a simulated moving bed system. The fixed bed employs an equilibrium stage model. It is observed that with long enough reactor length, the exit stream from the reactor is essentially at equilibrium composition, whereas in the case of a simulated moving bed in which the feed entry point is continuously switched to simulate the countercurrent movement high product purity and conversion higher than equilibrium value are obtained.

Acknowledgement—This work was supported by the Division of Chemical Sciences, Office of Basic Energy Sciences, U.S. Department of Energy, under contract number DE-AC02-76-ER02945.

NOTATION

A	strongly adsorbed species, component *A*
B	less strongly adsorbed species, component *B*
C	concentration in the fluid phase, mol/v
CMCR	countercurrent moving bed chromatographic reactor
Conv	conversion
g	gas
k	rate constant
k_{ai}	adsorption rate constant of component i
k_b	backward surface reaction rate constant
k_{di}	desorption rate constant of component i
K_e	reaction equilibrium constant, k_f/k_b
k_f	forward surface reaction rate constant
K	adsorption equilibrium constant, K_A/K_B
K_i	adsorption equilibrium constant of component i
L	length
MES	mesitylene
n	solid-phase concentration, mol/v
N	solid-phase saturation concentration
p	number of segments in section I
P	total number of plates
q	number of segments in section II
r	reaction rate
SCMCR	simulated countercurrent moving bed chromatographic reactor
t	time
t_S	time interval between successive switching of feed stream
TMC	1,3,5-trimethylcyclohexane
u_g	carrier gas velocity
u_S	velocity of solid phase
X	axial position

Greek letters

α	stoichiometric coefficients
β	ratio of pseudo-solid flow rate to carrier flow rate
γ	dimensionless fluid-phase concentration, KC
δ	dimensionless forward reaction rate constant
Δ	$1 + \gamma_A + \gamma_B$
ε	interparticle void fraction
ζ	pseudo-solid speed, switching speed
κ	fraction recycled
λ	dimensionless adsorption/desorption rate constant
μ	phase ratio
ξ	dimensionless axial position
σ	relative carrying capacity
τ	dimensionless time, t/t_S
υ	dimensionless solid-phase concentration

Suffixes (subscripts/superscript)

0	initial state
a, ads	adsorption
A	component A
b	backward
B	component B
d, des	desorption
eq	equilibrium
f	feed, forward
g	gas
i	component i
in	inlet
j	section j
k	kth iteration
m	mth stage, mth switching period
n	nth stage
r	reaction
S	switching
I	section 1
II	section 2

REFERENCES

Cho, B. K., Aris, R. and Carr, R. W., 1982, The mathematical theory of a countercurrent catalytic reactor. *Proc. Roy. Soc. London* **A383**, 147.

Egan, C. J. and Buss, W. C., 1959, Determination of the equilibrium constants for the hydrogenation of mesitylene. *J. phys. Chem.* **63**, 1887.

Fish, B. and Carr, R. W., 1989, Experimental study of the countercurrent moving bed chromatographic reactor. *Chem. Engng Sci.* **44**, 1773.

Fish, B., Carr, R. W. and Aris, R., 1986, The continuous countercurrent moving bed chromatographic reactor. *Chem. Engng Sci.* **41**, 661.

Fish, B., Carr, R. W. and Aris, R., 1988, Computer aided experimentation in countercurrent reaction chromatography and simulated counter-current chromatography. *Chem. Engng Sci.* **43**, 1867.

Petroulas, T., Aris, R. and Carr, R. W., 1985a, Analysis of a countercurrent moving bed chromatographic reactor. *Comput. Maths. Appl.* **11**, 5.

Petroulas, T., Aris, R. and Carr, R. W., 1985b, Analysis and performance of a countercurrent moving bed chromatographic reactor. *Chem. Engng Sci.* **40**, 2233.